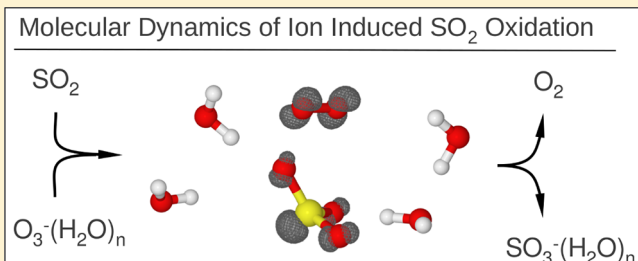


Reactions and Reaction Rate of Atmospheric SO₂ and O₃⁻(H₂O)_n Collisions via Molecular Dynamics SimulationsNicolai Bork,^{*,†,‡} Ville Loukonen,[†] and Hanna Vehkamäki[†][†]Division of Atmospheric Sciences and Geophysics, Department of Physics, University of Helsinki, Finland[‡]Department of Chemistry, H. C. Ørsted Institute, University of Copenhagen, Denmark

S Supporting Information

ABSTRACT: We present an ab initio study of gaseous SO₂ and O₃⁻(H₂O)_n collisions. Opposed to the usual approach to determine reaction rates via structural optimizations and transition state theory, we successfully approach this problem using ab initio molecular dynamics. We demonstrate the advantages of this approach, being the automatic and unbiased inclusion of dynamic and steric effects as well as the simultaneous assessment of all possible reactions. For this particular system, we find that only one reaction will be of atmospheric significance. Further, we identify the main geometrical parameters governing and limiting the observed reaction and suggest a new measure of the reaction rate being ca. 3/4 of the collision rate.

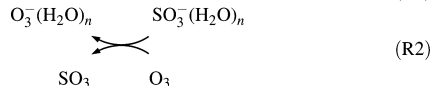


INTRODUCTION

Among the numerous trace gases in the atmosphere, sulfuric acid (H₂SO₄) is one of the most important. Sulfuric acid is known to play a decisive role in the earliest stages of new particle formation,¹ effecting both the radiative balance of the atmosphere² and cloud formation rates.³ Also, the chemical aging of many atmospheric organic species is dependent on pH, and high sulfuric acid concentrations can cause acid rain.⁴

The dominant source of atmospheric H₂SO₄ is gaseous SO₂. The rate limiting step is oxidation of SO₂ to SO₃, which is rapidly hydrated to H₂SO₄.⁵ Only two significant homogeneous mechanisms of SO₂ oxidation are currently known. The primary and most well-established mechanism is oxidation by OH radicals.^{6,7} More recently, it has been discovered that Criegee biradicals (R₁R₂COO) may contribute to SO₂ oxidation, especially in forested regions.^{8,9}

Complementary to both OH and Criegee based SO₂ oxidation, it has been proposed that some gaseous ions might catalyze oxidation of SO₂,¹⁰ e.g. via the reactions

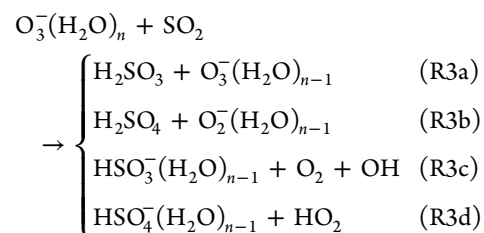


Besides O₃⁻, candidate ions include CO₃⁻, NO₂⁻, and N₂O⁻. The mechanism outlined in reactions R1 and R2 is backed up by recent ab initio studies^{11,12} and chamber experiments,^{13,14} although the present experimental evidence is mainly indirect.

Although ion induced catalysis may contribute to H₂SO₄ formation, it is presently not included in global models of atmospheric chemistry. The major hindrance is the lack of

knowledge about the underlying chemistry, preventing the overall catalytic efficiency from being determined.

Considering the first step in the mechanism, i.e., reaction R1, several side reactions are possible:



which may severely limit the catalysis. Although reaction R3a is slightly endothermic, all of reactions R3a–d are plausible outcomes of a collision between a hydrated O₃⁻ anion and SO₂ at standard conditions. Details on the thermodynamics of reactions R3a–d are presented in the Supporting Information.

To determine the importance of each of these reactions, a frequently used approach is to calculate the structures and energies of reactants, intermediates, products, and transition states. Hereafter, some kinetic model may be applied, and the absolute rates determined.^{15,16} However, a number of difficulties may arise, especially if a realistic number of water molecules are to be included, since the water molecules may adopt numerous configurations. Transition states are saddle points on the potential energy surfaces and are inherently more difficult to determine than the reactant and product structures,

Received: November 9, 2012

Revised: February 14, 2013

Published: March 8, 2013

which are local minima. Although several methods for systematic transition state searches exist, e.g., constraining coordinates or nudged elastic band techniques, the problem remains nontrivial.^{17,18} In this particular case, the transition states are most likely quite complicated since both O_3^- , SO_2 , and one or more H_2O may be involved.

To avoid these issues, we have undertaken an alternative approach via Born–Oppenheimer molecular dynamics (MD) simulations. By sampling a variety of $\text{SO}_2\text{--O}_3^-(\text{H}_2\text{O})_n$ collisions and determining their outcomes, several key properties have been deduced. Besides the product distribution, these include the effects of water, the nature of the impact, as well as dynamic and steric effects. Contrary to the traditional structure-optimization based approach, these results are by construction directly transferable to conditions in the atmosphere or in a reaction chamber. Finally, we provide a revised estimate of the reaction rate.

METHODOLOGY

Computational Details. Due to the complexity of the clusters, containing three different species all with relatively low symmetry (C_{2v}), as well as the need to study chemical reactions, only quantum based MD is suitable for this study. Although density functional theory (DFT)^{19,20} is not the most accurate and reliable ab initio method, this approach has a good trade-off between accuracy and computational expense and was thus chosen for this study. Also, DFT has successfully been applied in several related studies.^{16,21,22}

All MD simulations were performed using the Quickstep method²³ as implemented in the CP2K package (www.cp2k.org).^{24,25} Here, the wave function is described by atom-centered Gaussian basis functions of double- ζ polarized valence quality,²⁶ and the electronic density is described by plane waves truncated at 400 Ry. Core electrons are described by pseudopotentials.²⁷ Basis sets of double- ζ quality have been used in numerous related studies and generally yield a good compromise between computational expense and accuracy.^{28–30} Concerning the present reaction, we have previously compared DFT calculations of double- ζ basis set quality with explicitly correlated CCSD(T)-F12 calculations^{31,32} showing that discrepancies of 5–10 kJ/mol should be expected.¹²

Periodic boundary conditions were not used. Special care was taken to avoid unphysical cell boundary effects.¹⁶ We found that both the energy and the dipole moment of an optimized $\text{O}_3^-(\text{H}_2\text{O})_5$ cluster converged at cell sizes of $20 \times 20 \times 20 \text{ \AA}^3$, and hence this cell was used.

Since collision times with N_2 or O_2 at normal pressures are on the order of 150 ps,³³ the systems at hand will, in general, not experience any other collision than the investigated SO_2 impact within a typical simulation. Hence, the total energy of the systems should be conserved, and the simulations were performed in NVE ensembles. Different timesteps for the nuclear propagation were tested. We found that timesteps larger than 1 fs induced significant drift in the total energy of the system due to unphysical OH vibrations. Using a 1 fs time step reduced the drift to less than 0.05 kJ mol^{-1} per 3000 steps.

We have used the DFT functional by Perdew, Burke and Ernzerhof (PBE)³⁴ mainly since this functional, being a pure ab initio functional, outperforms hybrid DFT functionals concerning parallelization within the CP2K package. Also, several studies have previously compared the performance of various DFT functionals. Specifically aimed at atmospheric sulfur chemistry, a recent study by Elm et al. showed that especially

concerning energies PBE remains one of the most accurate functionals.³⁰

It is well known that dispersion is ill described by most DFT functionals. Although PBE is known to require less dispersion correction than, e.g., BLYP or B3LYP, the effects of dispersion have been tested using the D3 correctional scheme by Grimme et al.³⁵

All simulations were parallelized on 32 processors, and the calculations were run for 72 h or until a reaction had occurred. In about one-third of the simulations, the outcome was uncertain after 72 h. These simulations were extended by additional 72 h or until a decisive outcome could be determined. Typically, a 72 h run yielded between 2500 and 3000 MD steps.

The spin multiplicity was a concern since two of the possible reactions involved the formation of molecular oxygen. While the remaining species are singlets or doublets, it is well-known that molecular oxygen is a triplet. Therefore, a spin flip is required before the potential energy gain of O_2^3 formation is realized (ca. 95 kJ mol^{-1}).³⁶ However, the singlet to triplet oxygen transition is forbidden by orbital parity and spin, and the radiative lifetime of singlet O_2 is extremely long (72 min).³⁶ Hence, the production of singlet O_2 was enforced.

$\text{O}_3^-(\text{H}_2\text{O})_5$ Structures. To obtain realistic results, the structures of the reactants must be determined. The water affinity of O_3^- exceeds that of most other ions, and at least five, possibly more, water molecules will attach to O_3^- under typical atmospheric conditions.^{22,37} Due to computational expense, it is important to keep the systems as small as possible, and hence the $\text{O}_3^-(\text{H}_2\text{O})_5$ cluster was chosen as a model.

Even at temperatures considerably below $0 \text{ }^\circ\text{C}$, the hydrogen bonds are not strong enough to prevent reorientations of the water molecules, and thus multiple configurations coexist.²² On the basis of a previous series of simulated annealings,²² we chose to focus on two model systems. In one system, henceforth denoted “tight”, the water molecules form a strong network of hydrogen bonds resembling the ground state structure. In the other system, henceforth denoted “loose”, the water molecules form a looser network with higher internal energy but also larger entropy. Both clusters are shown in Figure 1.

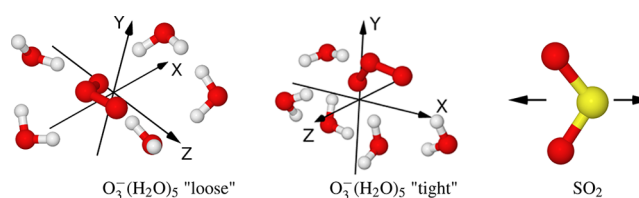


Figure 1. Configurations of the reactants also showing the three principal axis along which the collisions occur. The two impact orientations of SO_2 are indicated as well. Oxygen is red, hydrogen is white, and sulfur is yellow.

The Boltzmann entropy is given as

$$S_{\text{config}} = k_B \cdot \ln(W) \quad (1)$$

where k_B is the Boltzmann constant, and W is the number of microstates within a given macrostate, i.e. the number of configurations within a small energy interval. Although it is evident that W_{loose} exceeds W_{tight} quantifying ΔS_{config} remains nontrivial. However, for the two configurations to be equally probable, it is required that $W_{\text{loose}}:W_{\text{tight}} = 200:1$. Considering

that the number of stable configurations probably is less than 200 for either cluster, we conclude that $W_{\text{loose}} \cdot W_{\text{tight}} \ll 200:1$. Hence the reactivity and dynamics of reaction R1 at atmospheric conditions are dominated by clusters with tight water networks. Details on the thermodynamics including vibrational frequencies and further considerations of the effect of Boltzmann entropy are given in the Supporting Information.

Impact Directions and Velocity. Starting from optimized $\text{O}_3^-(\text{H}_2\text{O})_5$ geometries, the initial velocities of these atoms were determined by short (5–10 fs) MD simulations at a fixed temperature. The SO_2 molecule was not vibrationally excited but only given velocity in the direction of the impact. The impact velocities were determined assuming a Maxwell–Boltzmann distribution of speeds. The average relative speed is then given as

$$v_{\text{rel}} = \sqrt{\frac{8k_{\text{B}}T}{\pi\mu}} \quad (2)$$

where μ denotes the reduced mass, and T is the absolute temperature.³³

Preferably, we would start all simulations at energies corresponding to atmospherically relevant temperatures. However, we chose to increase the initial energy by applying $T = 500$ K. This significantly increased the reaction rates and hence reduced the required simulation time. Hereby, more simulations and a more thorough sampling of configurations and collision angles could be realized. A full scan of all collision angles is computationally extremely costly, and a selection must be made. In this study, we have focused on collisions where the incoming SO_2 collides at approximately the center of the $\text{O}_3^-(\text{H}_2\text{O})_5$ clusters. Two orientations of the SO_2 molecule were considered: one with the sulfur atom facing forward and the other with the oxygen atoms facing forward. Since the two chosen $\text{O}_3^-(\text{H}_2\text{O})_5$ clusters are not symmetrical, the impact angles were varied in a way that all sides of the clusters are hit. The clusters were randomly oriented in space and centered at the origin. The SO_2 molecules were placed between 4 and 5 Å from the cluster in 6 directions aligned with each of the Cartesian axis. Hence, in total, 24 simulations were run. All angles and axis are illustrated in Figure 1.

RESULTS AND DISCUSSION

The result of each simulation, its length and initial configuration are shown in Figure 1 and tabulated in the Supporting Information. Out of the 24 simulations, only three different outcomes were observed. The most frequent outcome was reaction R1, which occurred in 13 simulations. The second most frequent outcome was a nonsticking collision, which left the SO_2 and $\text{O}_3^-(\text{H}_2\text{O})_n$ species separated by 4–6 Å ngstroms, but with little further interaction. This occurred in eight simulations. The least frequent outcome was collisions where the SO_2 molecule was absorbed by the cluster, but where no reaction occurred in the investigated time period. This occurred in three simulations.

The effects of dispersion was tested in six simulations. Although adding dispersion did alter the outcome of a given simulation, we did not see any evidence of secondary reactions or outcomes different from the ones presented above. On the contrary, both nonsticking, sticking but nonreactive, and reactive collisions were observed. Dispersion forces remain a challenge for DFT, but the structures of most hydrated ions are generally governed by ion-dipole interactions and hydrogen

bonds. Hence, the effect of dispersion contribution is qualitatively negligible

Further, the effect of basis set superposition error (BSSE) was investigated, and a plot of BSSE as a function of simulation time is available in the Supporting Information. Since SO_2 and O_3^- interact strongly, we chose to investigate BSSE between O_3^-SO_2 and $(\text{H}_2\text{O})_5$ using the counterpoise method³⁸ on the geometries from the simulation also shown in Figures 3A and 4. Prior to SO_2 impacting the $\text{O}_3^-(\text{H}_2\text{O})_5$ cluster, BSSE was around 30 kJ mol⁻¹. After impact, BSSE was found slowly varying between 10 and 20 kJ mol⁻¹. Since the observed differences in BSSE are small and since BSSE is only slowly varying, BSSE is unlikely to either hinder or favor oxygen transfer. Omitting BSSE is thus not expected to induce any significant error.

Despite the forbidden spin flip, reaction R1 releases a significant amount of chemical energy. Until another species collides with the reactants, after ca. 150 ps on average,³³ this energy is conserved as vibrational and kinetic energy within the products. The main effect of this was an excited S–O vibration, and the rapid ejection of the O_2 molecule from the cluster. Two typical examples are shown in Figure 2, and the trajectories, in

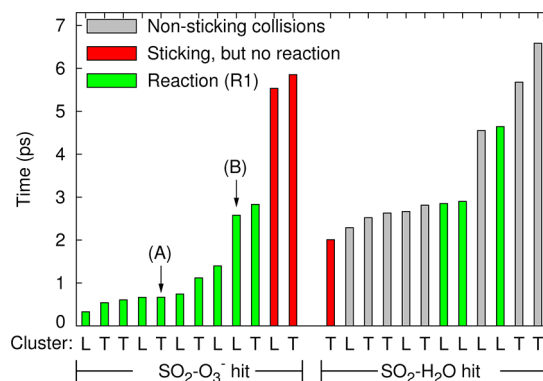


Figure 2. Summary of all simulations. When the initial hit was SO_2-O_3^- , the SO_2 was in all cases absorbed in the cluster and most often, reaction R1 occurred rapidly. When the initial hit was $\text{SO}_2-\text{H}_2\text{O}$, most often, SO_2 was not absorbed. The initial cluster configuration is indicated by “L” (loose) and “T” (tight). More details of the simulations denoted (A) and (B) are shown in Figures 3 and 4.

xyz format, and energies are available in the Supporting Information. It can be seen how the potential energy, after the initial collision and reorientations, suddenly drops about 100 kJ mol⁻¹ simultaneously with the decrease of the S–O distance as the bond is formed (see also Figure 4). Also apparent in Figure 4 are the fundamental changes of the electronic structure caused by the reaction. The net spin density clearly reveals that the extra electron initially and in the transition state is confined to an antibonding orbital on O_3^- . After the reaction, the charge is located on the SO_3^- and the antibonding π^* orbital of the singlet O_2 is apparent

The vibrational excitation of the bond is also apparent in Figure 3. Further, the nascent O_2 molecule is seen to rapidly leave the cluster at speeds exceeding 1 Å per 100 fs (1000 m s⁻¹). On a few of the reacting simulations, the effects of the spin flip were examined by taking a configuration immediately after the reaction, and continuing the simulation with triplet O_2 . However, this lead to no noticeable difference in the further fate of the reactant cluster.

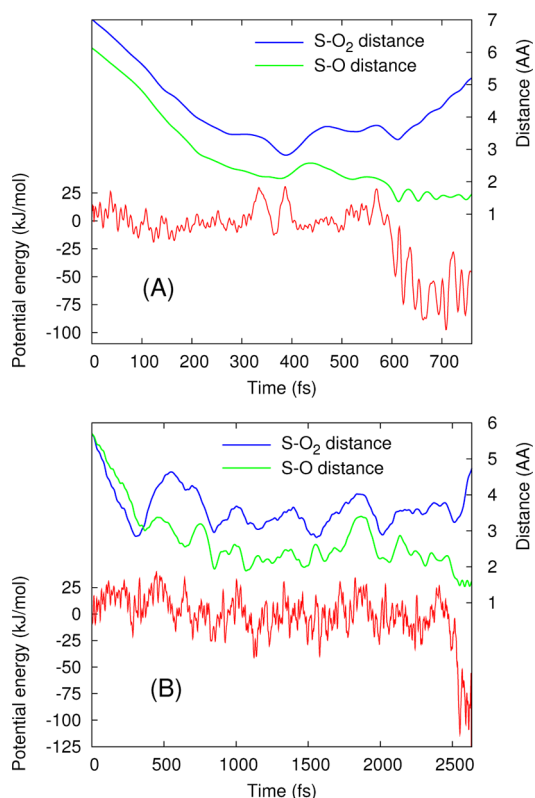


Figure 3. Potential energy and two descriptive distances as a function of time of two typical reactive simulations. Note the rapid increase of the S–O₂ distance after the reaction. For clarity, the plotted energies are 5-point averages. Trajectories in xyz format are given as Supporting Information. Some important configurations of simulation (A) are shown in Figure 4 where also the “S–O₂” and “S–O” distances are illustrated.

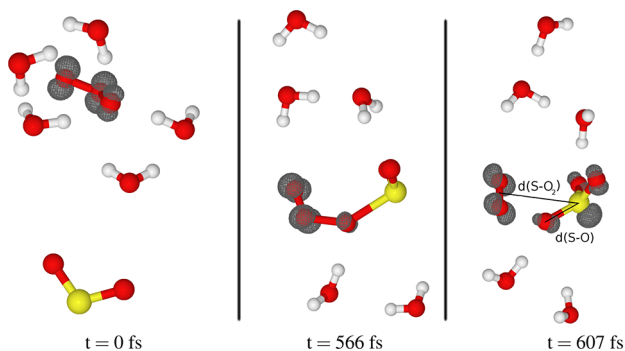


Figure 4. Selected structures of the run shown in Figure 3A. $t = 0$ fs corresponds to the initial configuration, $t = 566$ fs corresponds to the transition state, and $t = 607$ fs corresponds to newly formed products. The spin density is shown, and the π^* orbital of the singlet O₂ can be seen. Trajectories, in xyz format, and energies are given in the Supporting Information. Oxygen is red, hydrogen is white, and sulfur is yellow.

Concerning the further chemistry of SO₃[−], the ejection of the singlet O₂ is an important feature. It is known that the most likely fate of SO₃[−] is oxidation by O₂ to SO₅[−].³⁹ However, it may now be assumed that the formation of SO₅[−] takes place via normal O₂³ and not via the newly formed singlet O₂. Since the chemical properties of any molecule is highly dependent on its electronic state, this should be important for the further chemical development of the SO₃[−](H₂O)₃ cluster. We note that

the discovery of this effect comes naturally from the MD simulations but could not have been made using a standard geometry optimization approach.

Next, we examined the effects of the different collision sites and orientations. Several studies on sticking probabilities to water surfaces or water-based aerosols have been published. It has been found that the sticking probability of bulky organic species, such as phenol and succinic acid, depends on their orientation at impact.^{40,41} On the contrary, the sticking probability of smaller inorganic species such as H₂O and SO₂ have been found largely independent of the orientation at impact.^{42,43} In accordance with these studies, no significant effect of the initial SO₂ orientation was found here.

We then analyzed the effects of the actual hit, i.e., whether it was a SO₂–O₃[−] or a SO₂–H₂O hit, which is also shown in Figure 2. Here, a strong effect was found. In all simulations of SO₂–O₃[−] hits, the SO₂ was absorbed in the cluster and most often, a reaction took place almost instantly. This is in accordance with collision-limited rate constants for the dehydrated reaction found in experiments.³⁷ On the contrary, 3/4 of the simulations of SO₂–H₂O hits were nonsticking. This is in accordance with previous experimental and modeling results, concerning uptake of SO₂ on pure water droplets, finding sticking probabilities of 10–25%.^{43,44} The further fate of the nonsticking collisions remains somewhat uncertain. However, the distances between the SO₂ and O₃[−] (4–6 Å) at the end of the simulation runs are significant. We thus argue that the following N₂ or O₂ collision will, most likely, cause the SO₂ to be removed from the cluster rather than pushing it toward the cluster for a second impact.

The clear tendency toward a single reaction was somewhat surprising. However, we were thereby able to conclude that the main outcome at atmospheric temperatures most likely is reaction R1 and that all of reactions R3a–d will be of minor significance. We note that no tunnelling effects were included in this study. Proton tunnelling is vastly more important than oxygen tunnelling, but since no indications of proton transfer reactions were seen, even at $T = 500$ K, we conclude that no proton transfer reactions will be important at $T = 300$ K.

Although the sticking, but nonreactive collisions have not reacted yet, it is unlikely for SO₂ to evaporate from the cluster. These reactions may take significantly longer than we are able to sample, but we consider it is most likely that they also will terminate via reaction R1. This increases the total number of reactive collisions to 8 + 1 and 5 + 2 for the “tight” and “loose” model clusters, respectively.

Accumulating these results, we find that at standard conditions and with 90% confidence level, the reaction rate is between 50 and 90% of the collision rate. The overall reaction rate of reaction R1, r_{R1} , is dominated by the reactivity of the “tight” model cluster due to its higher concentration, and our best estimate is then

$$r_{R1} = (8 + 1)/12 \times Z \quad (3)$$

$$= 3/4 \times Z \quad (4)$$

where Z is the collision rate.

The reaction rate of this system has previously been experimentally determined by Fehsenfeld and Ferguson using the flowing afterglow technique.³⁷ They determined a reaction rate constant of 1.7×10^{-9} cm³ s, suggesting not only a collision limited reaction rate, but also a 10 Å collision cross section due to dipole-ion interactions. However, they did not

include any water. Recent ab initio calculations by Bork et al.,¹¹ including up to five water molecules, confirmed that collision limited reaction rates were likely. Further, a catalytic effect of water was found, but no dynamic effects were included.

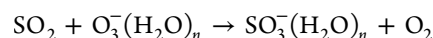
In the present study, both water and dynamic effects have been included. We find that, despite the catalytic effects previously found, the main effect of water is lowering the sticking probability and reaction rate by shielding the O_3^- ion toward the incoming SO_2 . Similarly, the ion dipole interaction between O_3^- and SO_2 is most likely also shielded by water. This further limits the reaction rates by lowering the collision cross section, although we currently are unable to quantify this contribution.

CONCLUSIONS

The oxidation of SO_2 to SO_3^- by $\text{O}_3^-(\text{H}_2\text{O})_n$ has been studied using ab initio MD simulations. We demonstrate the validity and strengths of this approach, which is the automatic inclusion of dynamic and steric effects, and the simultaneous assessment of all possible reaction pathways.

Two model clusters have been selected to represent two different, typical ground state structures. One is characterized by a dense water structure stabilized by hydrogen bonds, while the other is characterized by a looser water structure favored by higher entropy. SO_2 is brought to collide with the clusters from six directions along the Cartesian axis. Two orientations of the SO_2 molecule are used, leading to 24 simulations in total (see also Figure 1).

Three distinct outcomes were observed. Thirteen simulations lead to oxygen transfer as



Eight simulations did not lead to absorption of SO_2 in the cluster, thus being nonsticking collisions. Finally, three simulations lead to inclusion of SO_2 in the cluster but no chemical reaction in the simulated time interval. In no simulations were any side reactions observed. In all simulations where a reaction was observed, the newly formed O_2^1 molecule was rapidly ejected from the cluster due to the exothermicity of the reaction. Hence, the following formation of $\text{SO}_5^-(\text{H}_2\text{O})_5$ can be assumed to take place via normal O_2^3 .

We have studied several geometrical parameters with respect to their effect of the simulation outcome. We find that the orientation of the incoming SO_2 molecule is insignificant. However, the initial hit, either being SO_2-O_3^- or $\text{SO}_2-\text{H}_2\text{O}$, is significant. Most of the SO_2-O_3^- hits lead to rapid SO_3^- formation, while most of the $\text{SO}_2-\text{H}_2\text{O}$ hits lead to a nonsticking collision.

We use these results to improve the current estimates of the rate of reaction R1, and find it to be ca. 3/4 of the collision rate. Finally, we argue that the effective collision rate is most likely decreased by the water molecules by limiting the effects of the ion–dipole interaction.

ASSOCIATED CONTENT

Supporting Information

The following is included as Supporting Information: Thermodynamic data for reactions R3a–d, thermodynamic data for the two model clusters, an overview of all simulations including their runtimes and outcomes, and further considerations of the effect of Boltzmann entropy. A trajectory file in

xyz format. This material is available free of charge via the Internet at <http://pubs.acs.org>.

AUTHOR INFORMATION

Corresponding Author

*E-mail: nicolai.bork@helsinki.fi

Notes

The authors declare no competing financial interest.

ACKNOWLEDGMENTS

The authors thank the CSC-IT Center for Science Ltd. for computing time, the Academy of Finland (CoE Project No. 1118615, LASTU Project No. 135054), ERC (Project No. 257360- MOCAPAF), the Villum foundation, and the Maj and Tor Nessling Foundation for funding.

REFERENCES

- (1) Sipilä, M.; Berndt, T.; Petäjä, T.; Brus, D.; Vanhanen, J.; Stratmann, F.; Patokoski, J.; Mauldin, R., III; Hyvärinen, A.; Lihavainen, H.; Kulmala, M. The Role of Sulfuric Acid in Atmospheric Nucleation. *Science* **2010**, *327*, 1243–1246.
- (2) Solomon, S.; Qin, D.; Manning, M.; Chen, Z.; Marquis, M.; Averyt, K. B.; Tignor, M.; Miller, H. L. *IPCC, 2007: Climate Change 2007: The Physical Science Basis. Contribution of Working Group I to the Fourth Assessment Report of the Intergovernmental Panel on Climate Change, 2007*.
- (3) Rosenfeld, D. Aerosols, Clouds, and Climate. *Science* **2006**, *312*, 1323–1324.
- (4) Rodhe, H.; Dentener, F.; Schulz, M. The Global Distribution of Acidifying Wet Deposition. *Environ. Sci. Technol.* **2002**, *36*, 4382–4388.
- (5) Morokuma, K.; Muguruma, C. Ab Initio Molecular Orbital Study of the Mechanism of the Gas Phase Reaction $\text{SO}_3 + \text{H}_2\text{O}$: Importance of the Second Water Molecule. *J. Am. Chem. Soc.* **1994**, *116*, 10316–10317.
- (6) Li, W.; McKee, M. Theoretical Study of OH and H_2O Addition to SO_2 . *J. Phys. Chem. A* **1997**, *101*, 9778–9782.
- (7) Bondybey, V.; Beyer, M. How Many Molecules Make a Solution? *Int. Rev. Phys. Chem.* **2002**, *21*, 277–306.
- (8) Welz, O.; Savee, J.; Osborn, D.; Vasu, S.; Percival, C.; Shallcross, D.; Taatjes, C. Direct Kinetic Measurements of Criegee Intermediate (CH_2OO) Formed by Reaction of CH_2I with O_2 . *Science* **2012**, *335*, 204–207.
- (9) Mauldin, R., III; Berndt, T.; Sipilä, M.; Paasonen, P.; Petäjä, T.; Kim, S.; Kurtén, T.; Stratmann, F.; Kerminen, V.; Kulmala, M. A New Atmospherically Relevant Oxidant of Sulphur Dioxide. *Nature* **2012**, *488*, 193–196.
- (10) Svensmark, H.; Pedersen, J. O. P.; Marsh, N. D.; Enghoff, M. B.; Uggerhøj, U. I. Experimental Evidence for the Role of Ions in Particle Nucleation Under Atmospheric Conditions. *Proc. R. Soc. A* **2007**, *463*, 385–396.
- (11) Bork, N.; Kurtén, T.; Enghoff, M. B.; Pedersen, J. O. P.; Mikkelsen, K. V.; Svensmark, H. Structures and Reaction Rates of the Gaseous Oxidation of SO_2 by an $\text{O}_3^-(\text{H}_2\text{O})_{0-5}$ Cluster - A Density Functional Theory Investigation. *Atmos. Chem. Phys.* **2012**, *12*, 3639–3652.
- (12) Bork, N.; Kurtén, T.; Vehkamäki, H. *Atmos. Chem. Phys.* **2013**, *13*, 3695–3703.
- (13) Sorokin, A.; Arnold, F. Analysis of Experiments on Ion-Induced Nucleation and Aerosol Formation in the Presence of UV Light and Ionizing Radiation. *Atmos. Environ.* **2009**, *43*, 3799–3807.
- (14) Enghoff, M.; Bork, N.; Hattori, S.; Meusinger, C.; Nakagawa, M.; Pedersen, J.; Danielache, S.; Ueno, Y.; Johnson, M.; Yoshida, N. An Isotope View on Ionising Radiation as a Source of Sulphuric Acid. *Atmos. Chem. Phys.* **2012**, *12*, 5319–5327.

- (15) Kurtén, T.; Lane, J.; Jørgensen, S.; Kjørsgaard, H. A Computational Study of the Oxidation of SO₂ to SO₃ by Gas-Phase Organic Oxidants. *J. Phys. Chem. A* **2011**, *115*, 8669–8681.
- (16) Bork, N.; Bonanos, N.; Rossmeis, J.; Vegge, T. Thermodynamic and Kinetic Properties of Hydrogen Defect Pairs in SrTiO₃ From Density Functional Theory. *Phys. Chem. Chem. Phys.* **2011**, *13*, 15256–15263.
- (17) Olsen, R.; Kroes, G.; Henkelman, G.; Arnaldsson, A.; Jónsson, H. Comparison of Methods for Finding Saddle Points Without Knowledge of the Final States. *J. Chem. Phys.* **2004**, *121*, 9776–9792.
- (18) Henkelman, G.; Jóhannesson, G.; Jónsson, H. Methods for Finding Saddle Points and Minimum Energy Paths. *Theor. Methods Condens. Phase Chem.* **2002**, 269–302.
- (19) Kohn, W. Nobel Lecture: Electronic Structure of Matter-Wave Functions and Density Functionals. *Rev. Mod. Phys.* **1999**, *71*, 1253–1266.
- (20) Hohenberg, P.; Kohn, W. Inhomogeneous Electron Gas. *Phys. Rev.* **1964**, *136*, B864–B871.
- (21) Kurtén, T.; Sundberg, M. R.; Vehkamäki, H.; Noppel, M.; Blomqvist, J.; Kulmala, M. Ab Initio and Density Functional Theory Reinvestigation of Gas-Phase Sulfuric Acid Monohydrate and Ammonium Hydrogen Sulfate. *J. Phys. Chem. A* **2006**, *110*, 7178–7188.
- (22) Bork, N.; Kurtén, T.; Enghoff, M. B.; Pedersen, J. O. P.; Mikkelsen, K. V.; Svensmark, H. Ab Initio Studies of O₂⁻(H₂O)_n and O₃⁻(H₂O)_n Anionic Molecular Clusters, n ≥ 12. *Atmos. Chem. Phys.* **2011**, *11*, 13947–13973.
- (23) VandeVondele, J.; Krack, M.; Mohamed, F.; Parrinello, M.; Chassaing, T.; Hutter, J. Quickstep: Fast and Accurate Density Functional Calculations Using a Mixed Gaussian and Plane Waves Approach. *Comput. Phys. Commun.* **2005**, *167*, 103–128.
- (24) Lippert, G.; Hutter, J.; Parrinello, M. The Gaussian and Augmented-Plane-Wave Density Functional Method for Ab Initio Molecular Dynamics Simulations. *Theor. Chim. Acta* **1999**, *103*, 124–140.
- (25) Lippert, B.; Hutter, J.; Parrinello, M. A Hybrid Gaussian and Plane Wave Density Functional Scheme. *Mol. Phys.* **1997**, *92*, 477–488.
- (26) VandeVondele, J.; Hutter, J. Gaussian Basis Sets for Accurate Calculations on Molecular Systems in Gas and Condensed Phases. *J. Chem. Phys.* **2007**, *127* (114105), 1–9.
- (27) Goedecker, S.; Teter, M.; Hutter, J. Separable Dual-Space Gaussian Pseudopotentials. *Phys. Rev. B* **1996**, *54*, 1703–1710.
- (28) Seta, T.; Yamamoto, M.; Nishioka, M.; Sadakata, M. Structures of Hydrated Oxygen Anion Clusters: DFT Calculations for O⁻(H₂O)_n, O(H₂O)_n, and O(H₂O)_n (n = 0–4). *J. Phys. Chem. A* **2003**, *107*, 962–967.
- (29) Ortega, I.; Kupiainen, O.; Kurtén, T.; Olenius, T.; Wilkman, O.; McGrath, M.; Loukonen, V.; Vehkamäki, H. From Quantum Chemical Formation Free Energies to Evaporation Rates. *Atmos. Chem. Phys.* **2012**, *12*, 225–235.
- (30) Elm, J.; Bilde, M.; Mikkelsen, K. Assessment of Density Functional Theory in Predicting Structures and Free Energies of Reaction of Atmospheric Prenucleation Clusters. *J. Chem. Theory Comput.* **2012**, *8*, 2071–2077.
- (31) Adler, T. B.; Knizia, G.; Werner, H. J. A Simple and Efficient CCSD(T)-F12 Approximation. *J. Chem. Phys.* **2007**, *127* (221106), 1–4.
- (32) Werner, H. J.; Adler, T. B.; Manby, F. R. General Orbital Invariant MP2-F12 Theory. *J. Chem. Phys.* **2007**, *126* (164102), 1–18.
- (33) Atkins, P.; de Paula, J. *Physical Chemistry*; Oxford University Press: New York, 2006.
- (34) Perdew, J.; Burke, K.; Ernzerhof, M. Generalized Gradient Approximation Made Simple. *Phys. Rev. Lett.* **1996**, *77*, 3865–3868.
- (35) Grimme, S.; Antony, J.; Ehrlich, S.; Krieg, H. A Consistent and Accurate Ab Initio Parametrization of Density Functional Dispersion Correction (DFT-D) for the 94 Elements H–Pu. *J. Chem. Phys.* **2010**, *132* (154104), 1–19.
- (36) Schweitzer, C.; Schmidt, R. Physical Mechanisms of Generation and Deactivation of Singlet Oxygen. *Chem. Rev.* **2003**, *103*, 1685–1758.
- (37) Fehsenfeld, F. C.; Ferguson, E. E. Laboratory Studies of Negative Ion Reactions with Atmospheric Trace Constituents. *J. Chem. Phys.* **1974**, *61*, 3181–3193.
- (38) Boys, S.; Bernardi, F. The Calculation of Small Molecular Interactions by the Differences of Separate Total Energies. Some Procedures With Reduced Errors. *Mol. Phys.* **1970**, *19*, 553–566.
- (39) Möhler, O.; Reiner, T.; Arnold, F. The Formation of SO₅⁻ by Gas Phase Ion–Molecule Reactions. *J. Chem. Phys.* **1992**, *97*, 8233–8239.
- (40) Sloth, M.; Jørgensen, S.; Bilde, M.; Mikkelsen, K. Investigation of Particle–Molecule Interactions by Use of a Dielectric Continuum Model. *J. Phys. Chem. A* **2003**, *107*, 8623–8629.
- (41) Falsig, H.; Gross, A.; Kongsted, J.; Osted, A.; Sloth, M.; Mikkelsen, K. V.; Christiansen, O. Uptake of Phenol on Aerosol Particles. *J. Phys. Chem. A* **2006**, *110*, 660–670.
- (42) Ma, X.; Chakraborty, P.; Henz, B.; Zachariah, M. Molecular Dynamic Simulation of Dicarboxylic Acid Coated Aqueous Aerosol: Structure and Processing of Water Vapor. *Phys. Chem. Chem. Phys.* **2011**, *13*, 9374–9384.
- (43) Madsen, M. S.; Gross, A.; Falsig, H.; Kongsted, J.; Osted, A.; Mikkelsen, K. V.; Christiansen, O. Determination of Rate Constants for the Uptake Process Involving SO₂ and an Aerosol Particle. A Quantum Mechanics/Molecular Mechanics and Quantum Statistical Investigation. *Chem. Phys.* **2008**, *348*, 21–30.
- (44) Worsnop, D.; Zahniser, M.; Kolb, C.; Gardner, J.; Watson, L.; Van Doren, J.; Jayne, J.; Davidovits, P. The Temperature Dependence of Mass Accommodation of Sulfur Dioxide and Hydrogen Peroxide on Aqueous Surfaces. *J. Phys. Chem.* **1989**, *93*, 1159–1172.